### APART, A FIRST-ORDER DETERMINISTIC STRAY RADIATION ANALYSIS PROGRAM

Steven R. Lange, Robert P. Breault, and Alan W. Greynolds Optical Sciences Center, University of Arizona Tucson, Arizona 85721

#### Abstract

The APART code (Arizona's Paraxial Analysis of Radiation Transfer) is a deterministic stray radiation analysis program capable of yielding quantitative descriptions of systems along with insight into the scattering mechanism present. APART uses y-y geometrical optics to image primarily rotationally symmetrical systems. APART provides a sectional power map of the internal surfaces of a system and identifies "critical" objects seen from the image. Vane structures are modeled by configuration factors. Once the geometrical configuration factor between the internal objects has been calculated and stored, nonstructural changes to the system can be analyzed without re-running the complete program.

### Introduction

The problem of analyzing scattered radiation in a sensor system is difficult because of the multiplicity of object configurations among which scattered energy can be transferred and because of the variation of the scattering characteristics of the surfaces. Any quantitative analysis of scattered energy within a system will involve an overwhelming number of calculations. One solution to this problem is to minimize the number of calculations in a manner that develops user insight into the scattering mechanisms involved in the system. One does not want just a number at the end of the analysis but also the knowledge of the significant factors involved that make up the number and how system changes affect the number. APART was developed to separate the problem into a logical sequence of procedures and calculations that develops user insight for improvement of the system and to minimize the computational effort.

### Overview

APART is composed of three sub-programs called: Program One, Program Two, and Program Three, which together perform four functions. These programs (Figure 1) communicate with each other by disk files containing system information and the results of calculations. The programs can be run separately or in one job sequence. Program One contains the code for two separate calculations: a scan from the image and the image ing of all objects in each space. The remaining programs must be executed sequentially, although one program may be executed many times before the next is executed.

### Scan from Image

The first step in an APART analysis is to have the program "look out" from the image to determine which objects are seen either directly or in reflection. This calculation serves two functions: First, it will check for any design flaws that might be in the system. For example, one flaw might be an improperly designed baffle that allows energy from a stray radiation source to directly reach the detector. Program One scans from a selected image point outward to determine all objects that are seen from that image point. The program divides the length of the objects seen from the image into five sections and determines the position and angle at which each section is seen. APART also outputs a two-dimensional printer plot of the objects as they appear when projected onto the exit pupil of the system. With the combination of these outputs, one can quickly determine the status of the design. Redesign can take place at this point in the analysis at practically no cost to the user.

The second function served by Program One is to find the "critical" objects. These are the objects that scatter directly to the image and will be the sources at the final level of scatter. Thus, they have a "critical" effect on the system performance. The second to the last level of scatter is also partially determined; scattered radiation will be traced only to these "critical" objects. The final determination of the scattering paths is the linking of the objects that receive the initial unwanted energy to the critical objects, or to surfaces that scatter to the critical objects. A "level of scatter" is a scatter, or set of scatters, whereby radiation is transferred to another object. The other object may be the same one seen in reflection or even another part of the same object. Vane structure on an object will alter the number of scatters that will make up one level of scatter. The concept of levels of scatter is very important to the understanding of Program Three execution and will be explained further under "Program Three Calculations."

The scan from the image calculation is independent from the remainder of APART and can be rerun as many times as necessary to eliminate the design flaws or reduce the number of critical objects. Once the user is satisfied with the design as analyzed so far, he may continue the APART analysis.

# Imaging All Objects in Each Space

The purpose of this step in the APART analysis is to identify the power transfers to be calculated later in the analysis. For very simple systems without any optical elements, one can write these transfers without any computer analysis. However, when one is considering a system with several imaging elements, it is not clear whether an object can transfer power to another through several optical elements. Program One helps in

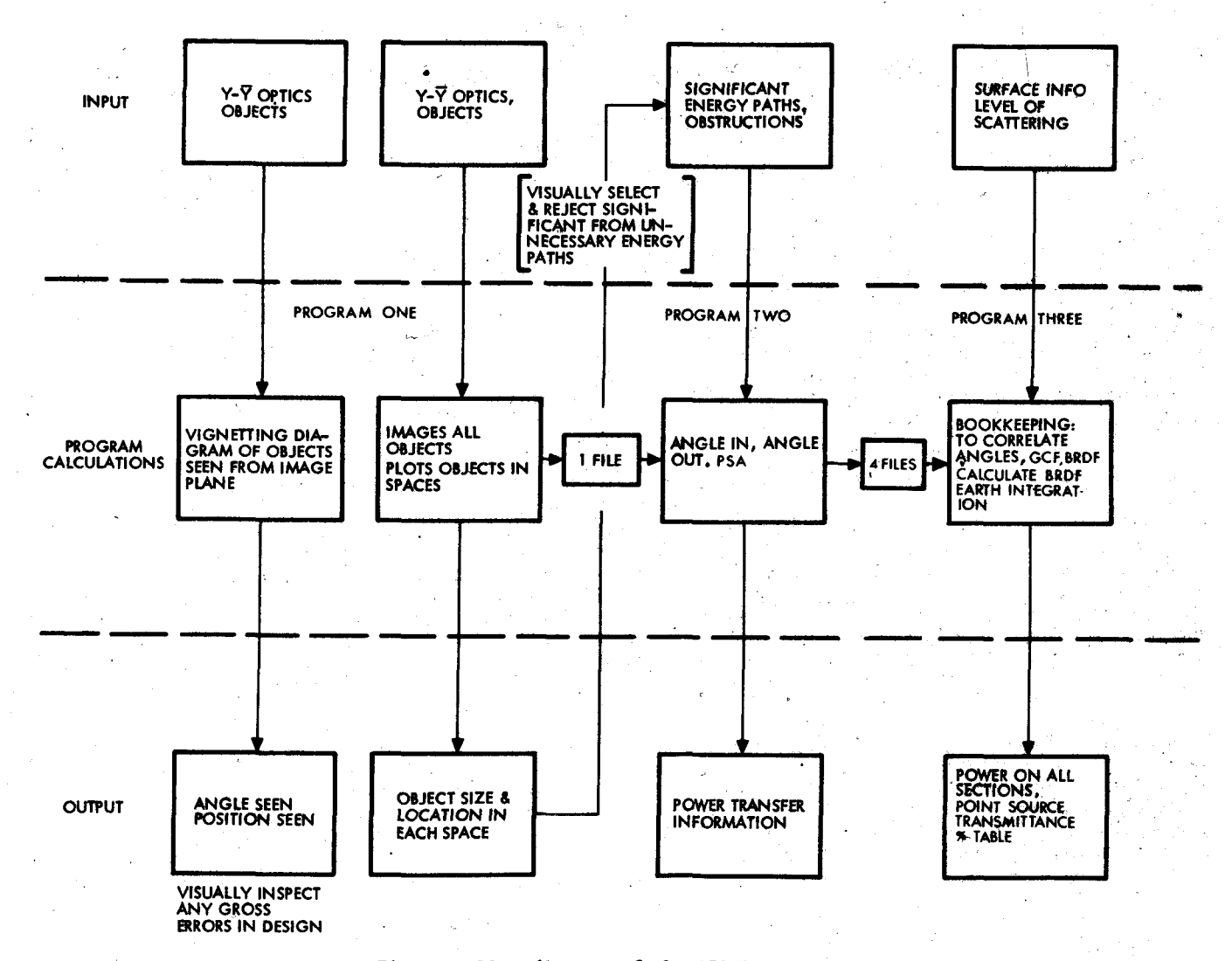


Fig. 1. Flow diagram of the APART program.

this determination by calculating the magnification and position of each object as it appears from each space within a system. The program plots this information from each space and, with the aid of a straight edge, can tell if power could transfer from one object to another. It is also easy to determine which objects might obscure any of the power to be transferred between the two objects. Several obscurations can block any or all of the beam, and these must be determined for input into the next program.

It is much more efficient to have the user select the objects that can be irradiated by the stray radiation source and select the paths that radiation can follow to reach the critical objects rather than have the computer blindly calculate every possible power transfer. By manually selecting the power transfers, one is doing a task quite simple for a human, and avoiding a very difficult, lengthy calculation for the computer. The other advantages in this interaction are that much computer time is saved by limiting the number of power transfers to be calculated, and the user gains insight into which power transfers are possible within a system and which surfaces can most influence the energy reaching the image.

# Y-Y Imaging Technique

Throughout Program One and Two imaging calculations are needed. To do this imaging, APART uses the first-order geometrical optics tool--the y-y diagram. (1,2) The y-y technique is much faster than other geometrical optical techniques. It allows the imaging of objects with a minimum of calculations regardless of the number of intervening imaging elements. APART must calculate the imaged location and the magnification of surfaces and obscurations to do the power transfer calculations. With the y-y technique, this is as simple as finding the intersection of two lines and calculating an area. Consider the y-y diagram for a simple mirror or lens with the object at minus infinity and the stop at the optical element (Figure 2). The distances between planes in the system, or points in the diagram, are given by the formula

$$t_{12} = n (y_1 \overline{y}_2 - \overline{y}_1 y_2) / \mathbf{R}$$
 (1)

where IK is the Lagrange invariant of the system and n is the index of refraction for the space in the

system or the line in the diagram.

Imaged heights are calculated by constructing a "conjugate" line from the origin through the point to be imaged to the line representing the space into which the object is to be imaged (Figure 3). The intersection of the conjugate line and the image line gives the y' and y' points of the imaged plane. The imaged distance can be calculated using Equation (1), and the magnification is given by the ratio of the y or y

$$\mathbf{m} = \mathbf{y'}/\mathbf{y} \text{ or } \overline{\mathbf{y'}}/\overline{\mathbf{y}}. \tag{2}$$

This technique is valid for any objects in any space within the system. Thus, the imaging involves quick calculations that avoid trigonometric and square root functions that are significantly more time consuming to calculate when compared to multiplication and division.

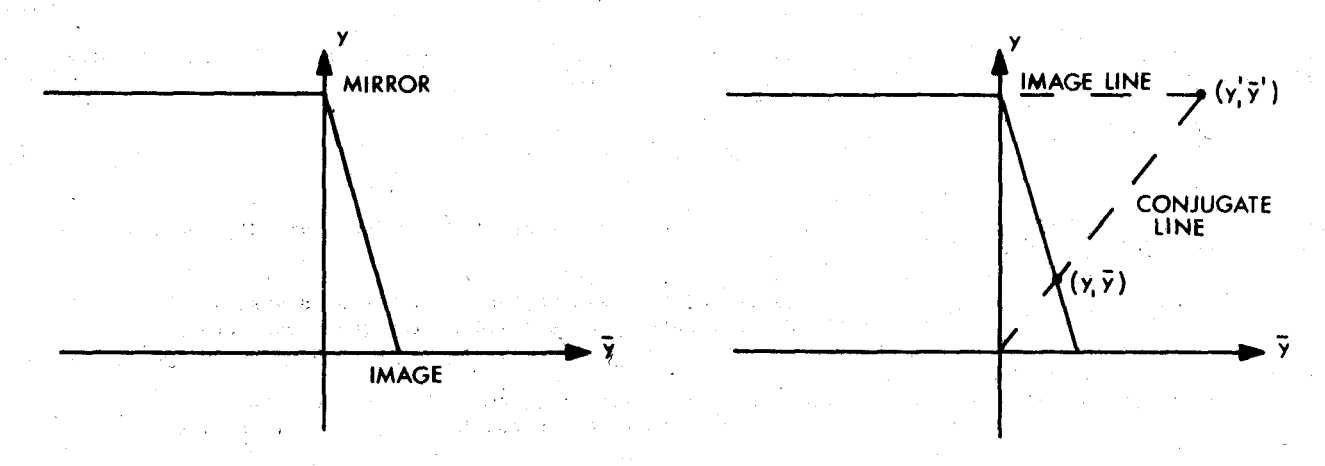


Fig. 2.  $Y-\overline{Y}$  diagram of a one-mirror system.

Fig. 3. Imaging of point  $(y, \overline{y})$  into space one.

# Power Transfer Calculations

Program Two calculates some of the factors leading up to the power transfer calculation in Program Three. Program Two divides all of the objects in the system into sections and if requested, into further subsections. APART calculates the power transfer from these sections to sections through the system to arrive at the total transferred energy.

# Power Transfer Equations

The equation that relates power transfer from one section to another is

$$dP_{c} = [L_{s}(\theta,\phi) dA_{s} \cos(\theta_{s}) dA_{c} \cos(\theta_{c})]/R^{2}_{sc}$$
(3)

where dP is the incremental amount of power transferred,  $L_g(\theta,\phi)$  is the bidirectional radiance of the source section, dA and dA are the elemental areas of the source and collector,  $\theta$  and  $\theta$  are the angles that the line of sight from the source to the collector makes with the respective surface normals, and  $\theta$  and  $\phi$  are the projected and azimuthal angles.

The total power P on the collector section is found by the integration in closed form of a double integral over the areas of the source and collector and then by the evaluation of the resultant algebraic expression:

$$P_{c} = \iiint \{ [L_{s}(\theta, \phi) \cos(\theta_{s}) \cos(\theta_{c})] / R^{2}_{sc} \} dA_{s} dA_{c}.$$
 (4)

APART does a numerical integration by subdividing the objects into elemental sections that are small when compared to the distance between them. The integrals are evaluated as sums over the source and collector sections:

$$P_{c} = \sum_{A_{c}} \sum_{A_{s}} \{ [L_{s}(\theta, \phi) \cos(\theta_{s}) \cos(\theta_{c}) \Delta A_{s} \Delta A_{c}] / R^{2}_{sc} \}.$$
 (5)

The bidirectional reflectance distribution function (BRDF) is defined as

$$BRDF(\theta_{i}, \phi_{i}; \theta_{o}, \phi_{o}) = \frac{L(\theta_{o}, \phi_{o})}{E(\theta_{i}, \phi_{i})}$$
 (6)

where  $E(\theta_i, \phi_i)$  is the bidirectional irradiance onto the source surface, and "i" and "o" refer to the incident (i) or scattered (o) direction of the ray. APART considers the radiance over the elemental area of the source as a constant and uses the BRDF to calculate the power incident on the collector as a function of the power incident on the source.

Multiplying and dividing Equation (3) by  $E(\theta_i, \phi_i)$  and dropping the angular dependence for convenience yields

$$dP_{c} = \int_{E}^{L} (E dA_{s}) \frac{\cos\theta_{s} \cos\theta_{c} dA_{c}}{g^{2}}.$$
 (7)

Equation (7) has been separated into three terms that can be rewritten as

$$dP_{c} = BRDF dP_{s} GCF. (8)$$

One can recognize the BRDF [as defined in Equation (6)] and  $dP_s$  as the power on the incremental source area and a new term called the geometrical configuration factor (GCF):

$$GCF = \frac{\cos\theta_{s} \cos\theta_{c} dA_{c}}{R^{2}}.$$
 (9)

When the power transfer equation has been written in the three-part form of Equation (8), the following qualitative statements can be made:

- 1) When only the coatings (BRDF) are varied to evaluate their effects on a system, the GCF does not change and it can be calculated once and stored for subsequent analysis.
- 2) When the system is not changed and only the source off-axis angle is altered in the analysis, the GCF remains fixed.
- 3) If an object in a system is altered in its size or shape, only transfers to or from this object, or transfers where it was used as an abscuration will need to be recalculated.

Program Two calculates the GCF between all previously determined source-collector combinations. Program Two also calculates and stores the angle information necessary for the calculation of the BRDF in Program Three. Thus, by storing this information, the computer time to do a number of analyses of a system is reduced tremendously.

Program Two divides objects into pi sections and axial, or z, sections. The reasons for this type of division will become apparent when symmetry rules are used. The program could divide the objects into hundreds of sections, but the storage problems in core become insurmountable, so APART limits the number of divisions of an object to 66. If more accuracy is desired, each section of each object may be further subdivided into as many subsections as one desires. Figure 4 illustrates how a cone can be divided. The result of the angle and GCF calculation between the subsections is averaged over one section-to-section transfer and stored for Program Three's use. Thus, problems such as accurately determining the shadow of a cone onto a cone can be handled with as much accuracy as desired.

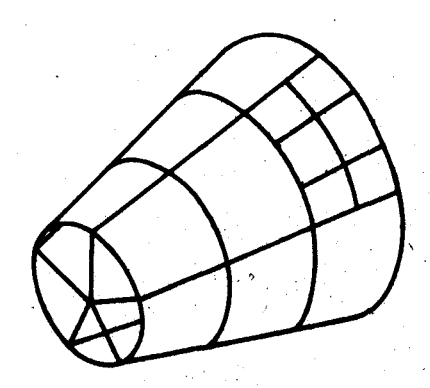


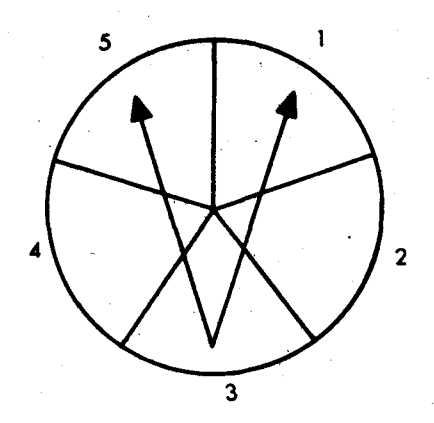
Fig. 4. Sections and subsections on a cone.

### Symmetry Considerations

When objects within a system are rotationally symmetrical about the optical axis, APART can use the symmetry to further reduce the necessary GCF and angle calculations. One can see in Figure 5a that the transfer from pi section three to pi section one involves only an angle sign change from the pi section three to pi section five transfer. This use of symmetry eliminates 2/5 of the calculations. Furthermore, the above

#### APART, A FIRST-ORDER DETERMINISTIC STRAY RADIATION ANALYSIS PROGRAM

use of symmetry can be rotated, as in Figure 5b. The above transfers are the same as the transfer from pi section two to pi sections four or five. Thus, to completely specify a power transfer between objects with one z section and five pi sections, only three calculations are necessary. Twenty-five calculations would be necessary for similarly sectioned objects that were asymmetrical.



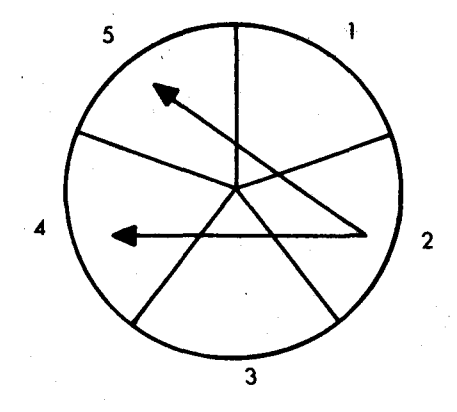


Fig. 5a

Fig. 5b

APART also uses this same type of symmetry when calculating the subsection-to-subsection transfers. Symmetry occurs here when the number of pi subsections on the source section equals the number of pi subsections on the collector section. This use of symmetry reduced the computer time for a three-by-three subsection transfer to about half of what it would have been with no symmetry.

#### Obstructions

Program Two considers obstructions when calculating the GCF. The obstructions, imaged or not, are handled in essentially the same manner as imaged objects. The vector from the source point to the collector point is used to determine the (x,y) intercept in the plane of an aperture or disk, where the intercept must be respectively inside or outside for power to pass. All obscurations are handled in a binary manner for the transfer between subsections to subsections. However, the average over a section-to-section transfer will result in a more realistic determination of the shadow. Obstructing conical sections pose additional problems because of their three-dimensional character. A ray now has the possibility of being blocked, passing around the cone, or passing through the cone. If the ray passes through both ends of the cone, the ray is not obstructed. Obviously, if the ray passes through one end and not the other, it fails. For the last case of a ray passing outside both cone ends, a further check must be made: from the source point, two planes can be drawn tangent to the obstructing cone, establishing a trapezoidal plane in space when intersected with the two cone ends. The ray is now checked for its position inside or outside of the trapezoid and, in conjunction with the other two tests, will determine the power transfer.

Now that the power transfers have been identified and the GCF and angle information for them calculated and stored, the APART analysis needs to calculate the remaining terms in Equation (8) and determine the resultant scatter throughout the system.

# Program Three Calculations

Program Three has two main functions: to calculate the BRDF for each section within the system for the angles needed and to calculate the power increments throughout the system. The result is the amount of power on all of the objects and insight into how this power got there.

# Surface Scatter Calculations

APART can accept BRDF values for a surface in a number of ways. First, actual data can be input in a tabled form. The data will be linearly interpolated for the angles actually encountered in Program Three. Second, the program can use any one of several models for the BRDF of the surface. The accuracy and speed of the models over the table lookup approach depend upon the coating, the cost, and the time to make sufficient measurements to fill the table.

The simplest model for surface scatter is a Lambertian model. Here, one inputs the total hemispherical reflectivity of the surface as a coating type for the surfaces on which it is to be used. The BRDF term in Equation (8) is a constant, and the calculation is finished. Because Lambertian scattering needs no angular information in Program Three, one can have Program Two ignore the lengthy surface angle calculations for these transfers, saving even more computer time.

Laboratory measurements of mirror surfaces have tended to indicate that a "smooth" mirror surface has a well-behaved linear shift-invariant BRDF function. (3) This function is linear when plotted on log-log paper with the ordinate being the BRDF and the abscissa being  $(\beta-\beta_0)$  where  $\beta$  is the sine of the angle of scattering and  $\theta_0$  is the sine of the specular angle. A typical example is shown in Figure 6. The program models this

function by reading in the ordinate intercept at  $\beta-\beta_0=0.01$  and the slope as plotted on the log-log paper. Average observed data can be input, or the results of a measurement program on the actual mirrors in a sensor can be used if the data are plotted and input as described.

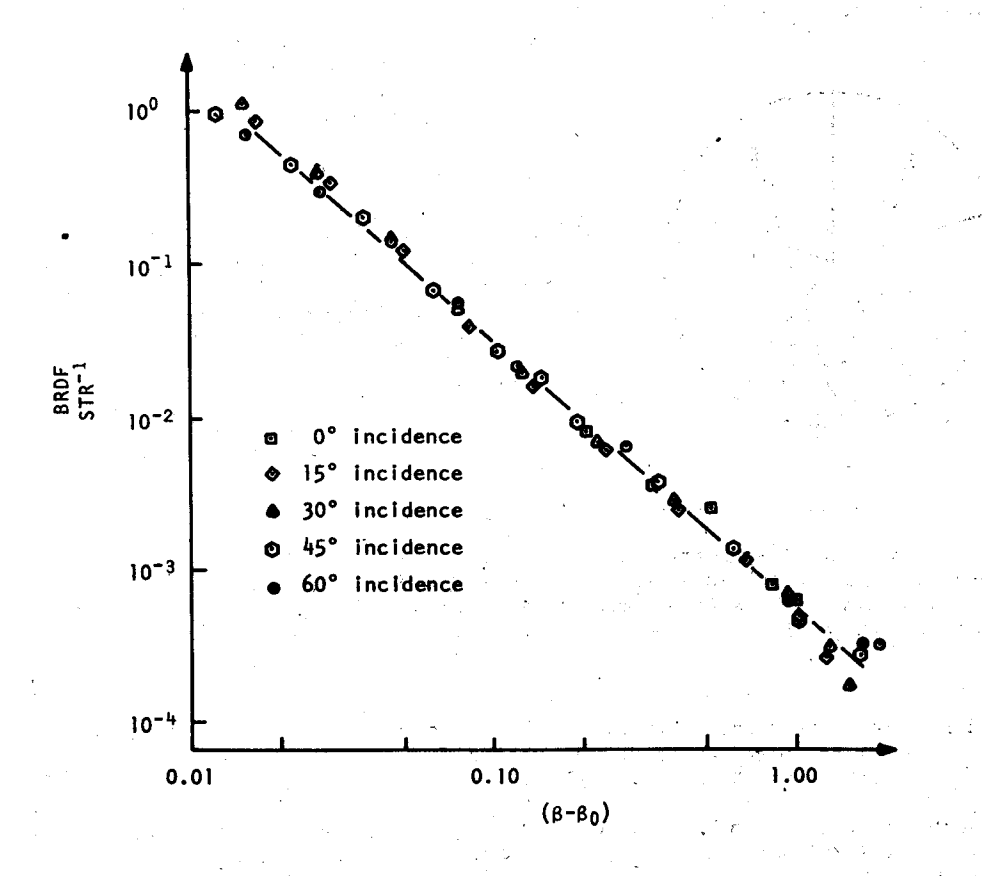


Fig. 6. BRDF of an average mirror.

For rougher surfaces that do not follow the linear shift-invariant properties observed on mirrors, there is a model called "blacks." This routine also utilizes data plotted in the Harvey-Shack manner described for the mirror surfaces above. These types of coatings are more similar to diffuse black surfaces like Martin Black or 3M Black Velvet than they are to mirrors. Measured data from these types of surfaces indicate that the slopes and starting points for small angle scattering change with the incident angle. Thus, the input for the program model includes a factor for the change in slope as a function of the incident angle and a factor for the change in BRDF at  $\beta$ - $\beta$ 0 = 0.01. The calculations for this type of model are much longer than for the Lambertian model, and this model is intended to be used as a final analysis tool for a very accurate description of a sensor.

The addition of vanes to a surface is handled in a unique fashion. Up to this point in the analysis, all surfaces were treated as cylinders or disks. Cones that have vanes designed onto the baffle cones are considered to be conical sections with the cone being located at the locus of vane tips. Vanes could be handled by inputting each side of a vane as a disk, with a cylinder to separate the vanes. This would include a large number of objects in the system and a tremendous number of angle and GCF calculations in Program Two. Vanes, as handled by APART, need only one angle and GCF calculations per section. Program Three knows, for a given transfer, what the angle into the surface and the angle out of the surface will be. For the vaned surface, as well as any other model, the program calculates the apparent reflectivity of the surface for those angles. To handle vaned surfaces, Program Three utilizes configuration factor geometry to calculate the power transfers within the vanes resulting in the BRDF of the vaned section. Thus, APART replaces a vaned object with an equivalent nonvaned surface that has an associated highly unsymmetrical BRDF. The input parameters necessary to describe a vaned surface include: the angle at which the vanes are tilted, their depth below the locus of vane tips, their spacing, their diffuse reflectivity, and their distance from the optical axis.

All vaned surfaces will have edges on the vanes, and these edges are also handled in a unique manner. As was previously mentioned, APART knows the angle radiation is hitting a surface, and the angle radiation will leave the section on its way to the collector. Thus, for a toroidal edge, the illuminated and "seen" part of the edge can be easily calculated. The arc length of the overlap can also be calculated. The arc length, along with a correction factor for the angle at which the illuminated portion of the edge is seen, is assumed to be a cylinder just as in the vaned surface calculation. An apparent reflectivity is calculated for the small cylinder representing the arc length and is added to the vane reflectivity as calculated above. Thus, all edges within a system are calculated in a deterministic manner. The input parameters for this surface

#### APART, A FIRST-ORDER DETERMINISTIC STRAY RADIATION ANALYSIS PROGRAM

model are the diffuse reflectivity of the edges and the radius of curvature of the edge tip. APART can handle different reflectivities and edge radii for vane tips located in different sections of the same object.

Thus, APART can utilize a variety of measured data to calculate the BRDF of the surfaces. Now two of the variables in Equation (8) have been calculated for a given section-to-section transfer. All that remains in the analysis is to have the program cycle through all of the object's sections and accumulate the result from Equation (8).

### Power Increments

The remaining term in Equation (8) to be calculated is dP. To start the calculations in Program Three, one must assign some starting amount of power onto some source(s) section. This initialized source may be a point located some distance from the entrance port of the system, if one is seeking to find a point source transmittance (PST). APART contains a simple loader routine that can load any or all sections of three objects with power. More sophisticated loader routines can be written that will include unusual obscurations or other situations not included in the general program.

The user must now enter the source-collector combinations as a function of the levels of scatter into Program Three. For example, at level one scatter the sources will be the objects that were loaded with the initial power. The collectors at level one scatter are all of the objects to which the sources can transfer power. The GCF's and angles for these transfers, as calculated in Program Two, must be recalled for this transfer calculation. The program will calculate dP for each source and collector section of the input combinations. Each increment of power reaching a collector section is stored separately and also is added after all power from all sources has been calculated. Thus, at the end of a level of scatter calculations, the program will have stored all increments of power to all the collectors and the total amount of power on each section of the collectors.

At the next level of scatter calculations, the above collectors will become sources. The sum of the increments of power on the collectors [Equation (5)] will become the dP of Equation (8). This sequence of calculations will continue until the image is a collector. The calculations can be carried out to a higher level of scatter if one wishes, but usually the energy reaching the image at the higher level is considerably lower than that received at a lower level of scatter.

One source section may contribute increments of power to the same collector section by several optical paths (i.e., directly or by reflection). When this power is then scattered from the collector into a single direction toward a second level collector, each increment of power incident on the first collector will contribute a different proportion of the scattered energy because of the different input angles. This is because the BRDF is generally angle dependent. Although the separate storage of these increments of power is a necessary and laborious task, it is responsible for the user's insight into the system scattering mechanisms.

The program can output a map of the increments of power reaching any object the user wishes. Of particular interest is a map of objects contributing power to the image. If a particular critical object is a major contributor of power, one can tell at a glance which sections on that critical object contributed the most power. Tables 1 and 2 illustrate some of the output from Program Three for two objects transferring power to the image.

Table 1. Power on One Section of the Image Coming from the Main Tube This object is considered to the image

This is the power on pi section 3, z section 1

0	0	0	0	0.18E-06	Total	=	1.83E-07
0	0	0 1	0	0	Total	=	0
0	0	0	0	0	Total :	=	0
0	0	0	0	0	Total :	=	0
0	0	0	.0	0.18E-06	Total :	= '	1.83E-07
<u>0</u>	₫ '	<u></u>	ō	3.67E-07			

Total power to this section is 3.67E-07.

Total

To

# Table 2. Power on One Section of the Image Coming from the Primary Mirror

This object is considered to the image

This is the power on pi section 3, z section 1

	0.38E-08	0.37E-08	0.37E-08	0.36E-08	0.35E-08	Total	=	1.84E-08
	0	0	0	0	0	Total	=	0
1,2	0	0	0	0	0	Total	==	0
	0	0	0	0	0	Total	=	0
	0.38E-08	0.37E-08	0.37E-08	0.36E-08	0.35E-08	Total	=	1.84E-08
otal	7.62E-09	7.49E-09	7.36E-09	7.23E-09	7.10E-09			• • •

Total power to this section is 3.68E-08

There will be one array of this type for each section of the image and one group of arrays from all objects transferring power to it. The numbers in the arrays contain the increments of power incident on the image from each section of the source listed. In the examples shown, the source objects have five pi and z sections each. For example, the power incident on the image from the primary mirror's pi section one and z section four is 0.36E-08. The user could now realize that only two sections of the main tube transfer power to the image compared to 10 sections from the primary mirror. Furthermore, the power coming from the main tube is about 10 times higher than from the primary mirror. Thus, for the data presented, the significant path is from the fifth z section of the main tube to the image. One can also request that the increments of power to the critical objects be printed. In this manner, the user can trace all of the scattered radiation throughout the system and identify the radiation from the significant paths followed to reach the image.

The user, having identified the important scattering paths, now has available the possible alternatives to improve the system performance. First, one can rerun only the significant paths and vary the surface coatings on the critical objects to determine their effects. It is important to realize that the addition of coatings or vanes on a surface does not mean that all of APART must be rerun with new input throughout. All that must be done is to change one card of the Program Three input deck and rerun Program Three. This step can also be done in the same job sequence by stacking runs. If the result of this step does not result in sufficient system improvement, one can consider the possible redesign of the system to eliminate the sections of the critical objects from the view of the image. Rerunning the Program One scan from the image will be helpful in this procedure. A third possibility is to alter the radiation incident on the most important sections of the critical objects. If the power reaching the critical sections can be lowered by system redesign or surface coatings, the power on the image likewise will be reduced. Thus, with the use of APART the user knows just which steps are possible to alter the system performance.

### Program Output

There are numerous output options available to the user of Program Three. The printing of the map of the power increments mentioned above is an example of a very detailed output. At the termination of each level of scatter, a running total of the power distribution on each object and the power incident at this level can be printed. Following all of the levels of scatter, a table of objects contributing power to the image can be output. This table lists the percent of the total energy reaching the image at each level of scatter from each object and the total power reaching the image at each level (Table 3). This percent table gives the user immediate insight into which objects are prime contributors and at what level they are; however, the knowledge of which sections of these objects are the most significant is lost in this output.

Table 3. A Percent Table for 3 Levels of Scatter

Percent of Power Contributed by Each Object as a Function Each Scattering Level

Objects	L	evel of Scatt	er
1 Source	1	2	3
2 Main Tube	0.0	0.0	0.0
3 Outer Secondary Baf	0.0	2.4	100.0
4 Inner Secondary	0.0	0.0	0.0
5 Outer Conical	0.0	0.0	0.0
6 Inner Conical	0.0	0.4	0.0
7	0.0	~ 0.0	0.0
8 Secondary Backing	0.0	0.0	0.0
9 Secondary Mirror	0.0	0.0	0.0
10 Primary Mirror	0.0	58.2	0.0
11 Entrance Port	0.0	39.0	0.0
12 Image Plane	0.0	0.0	0.0
13 Dummy	0.0	0.0	0.0
Total Power	0.0	0.477E-04	0.879E-0

\*Representative Cassegrain Stray Radiation Analysis

Following the calculation of all levels of scatter for an off-axis source angle, the program can store information for comparison with other source angles. An accumulated percent table can be stored for up to 10 source angles. This table includes the total energy reaching the image and the percent of energy coming from each of the objects in the system making up that total. Thus, the user can see how the energy reaching the image changes with different off-axis source angles.

A figure of merit for the stray radiation rejection performance of the system called point source transmittance (PST) can be defined for each off-axis point as either

$$PST = \frac{Power/unit area on image}{Power/unit area at entrance port perpendicular to source}$$
(10)

$$PST = \frac{\text{Total power on image}}{\text{Total power on entrance port}}.$$
 (11)

These PST's can be stored for each source angle and plotted against the off-axis angle at the end of a cycle of source angles. The plot can be either a printer plot or a Cal Comp plot.

Cycles of source angles can also be stacked in a single job execution. For example, one could run 10 source angles on a system with 90° baffle vanes on the main tube, alter the vane angles to 60°, and have the program plot both sets of results together. Up to eight cycles of source angles can be overplotted in one job execution. Parametric studies of the surface coatings as well as the effect of the BRDF on a system's performance can be made with very little setup time.

### Earth Integration

With the generated PST data, the contribution from a broad source can be integrated by subdividing the source and determining the off-axis angle for each section. The PST curve can be interpolated and a resulting irradiance on the image calculated. Such a routine, written by Gary Hunt, Sperry Support Services, Huntsville, Alabama, has been incorporated into APART. It is designed to integrate the radiation from an earch-shaped object for a set of earth limb angles designated in the input. The PST values are spline interpolated for the off-axis subsections of the earth. The irradiance on the earth, albedo, earth's radius, orbital altitude, and look angles to the hard earth are input variables. Output is the irradiance on the image and the total power reaching the image as a function of a set of earth limb angles.

### Comparison with Measured Data

The true value of an analysis program is measured by how accurately it predicts the real result. APART predictions have been compared to systems tested for their stray radiation rejection, and the results have usually been within a factor of two. The complex HOST sensor has been analyzed with APART (4) and the results have given us insight into how simple the scattering mechanisms can be, even in a complicated system. One system, a 0.5-m-diameter model of the Large Space Telescope (LST) has been designed, analyzed, fabricated, and tested to help determine APART's worth. Before testing started, an analysis of the system in its testing chamber revealed that the testing chamber was going to have a major influence on the amount of power reaching the image. As a result, the testing procedure had to be redesigned. The measured values gave very good agreement with the computer predictions. (5) The APART analysis was also helpful in directing the debugging of the test procedures.

# Conclusion

The APART program has been written to analyze the stray radiation in optical systems. It was designed to be straightforward in structure with a versatile output and a simple nonredundant input. It gives the user an excellent insight into the scattering mechanisms present within a system and also a clear understanding of how to improve the system for better stray radiation performance. APART uses a minimum of computer core and central processor time because it stores the results of calculations to eliminate unnecessary recalculation. Its ability to accurately predict the system performance as well as its ability to develop user insight have dispelled some preconceived notions about scattering principles.

# References

- 1. Delano, E., "First-Order Design and the y,y Diagram," Appl. Opt., Vol. 2, No. 12, pp. 1251-1256. 1963.
- 2. Shack, R. V., "Analytic System Design with a Pencil and Ruler--The Advantages of the y-y Diagram," Proc. SPIE, Vol. 39, Aug. 1973, Applications of Geometrical Optics.
- 3. Harvey, J. E., "Light-Scattering Characteristics of Optical Survaces," Ph.D. Dissertation, University of Arizona, 1976.
- 4. A Study Leading to Improvements in Radiation Focusing and Control in Infrared Sensors, Final report for D/A project 8X363304D215, Report No. AMMRC CTR 76-42, Army Materials & Mechanics Research Center, Watertown, Mass., 02172.
- 5. Hunt, G. H. and Shelton, G. B., "Experimental Measurement and Computer Analysis of Stray Radiation in a Telescope," in Proc. SPIE, Vol. 107, April 1977.